Carcinogenesis vol.10 no.3 pp.419–427, 1989

The chemistry and biology of 7H-dibenzo[c,g]carbazole: synthesis and characterization of selected derivatives, metabolism in rat liver preparations and mutagenesis mediated by cultured rat hepatocytes

David B.Stong[1], Robert T.Christian[2], Koka Jayasimhulu[2], R.Marshall Wilson[3] and David Warshawsky[2,4]

[2]Department of Environmental Health, University of Cincinnati Medical Center, Cincinnati, OH 45267, and [3]Department of Chemistry, University of Cincinnati, Cincinnati, OH 45221, USA

[1]Present address: Eastman Pharmaceuticals, 25 Great Valley Parkway, Great Valley, PA 19355, USA

[4]To whom all correspondence should be sent

Authentic stable standards of 7H-dibenzo[c,g]carbazole (DBC), a potent environmental carcinogen, were synthesized in order to study the compound's metabolism and mutagenesis in whole cell systems. Complete characterization of 2-OH-DBC, 3-OH-DBC, 4-OH-DBC, 13c-OH-DBC and *N*-methyl-DBC was accomplished by UV, IR, fluorescence and high resolution NMR spectra, and by high resolution mass spectrometric procedures. Metabolites of DBC were isolated and separated by HPLC from extracts of rat liver microsomal incubations and the medium of primary cultures of rat liver cells. Identification of metabolites was accomplished by comparisons between the authentic standards and isolated metabolites by UV and fluorescence spectroscopy, mass spectral analyses, and by co-chromatographic techniques. 2-OH-DBC and 3-OH-DBC were found in all rat liver preparations as well as three other unidentified phenols. 4-OH-DBC, 13c-OH-DBC or *N*-methyl-DBC were not isolated under any conditions. The rates of appearance of DBC metabolites in cultures of rat liver cells were compared to those for benzo[a]pyrene (BaP) at 10, 25, 50 and 100 μM substrate. At 25 μM substrate or greater, DBC metabolites appeared in the culture medium at significantly faster rates than those of BaP. At 100 μM substrate, DBC metabolites appeared at a rate ~4-times the rate observed for BaP. When the mutagenic potential of DBC was compared to that of BaP under identical conditions in a co-cultivation system of rat liver cells and an epithelial cell line, DBC was found to produce significantly higher rates of mutagenesis than BaP at concentrations of 0.4, 4.0 and 40.0 μM in the culture medium. The mutagenic potential of DBC was compared to that of several derivatives of the parent compound. 3-OH-DBC, 13c-OH-DBC and *N*-methyl-DBC were found to be mutagenic in the co-cultivation system at 40 μM, with mutation frequencies of 4.4 ± 0.8, 8.0 ± 3.1 and 12.9 ± 5.4 mutants per 10^5 survivors, respectively. The parent compound induced 8.0 ± 2.8 mutants per 10^5 survivors at the same concentration. 2-OH-DBC and 4-OH-DBC were not mutagenic under the same conditions. The studies have shown that metabolism of 7H-DBC leads predominantly to phenols in rat liver cells. The results of the mutagenesis experiments indicate that, of the derivatives studied, those associated by induction to the nitrogen are mutagenic. The latter studies suggest that the nitrogen is involved in the activation of the parent compound through inductive mechanisms.

Introduction

7H-Dibenzo[c,g]carbazole (DBC*) (Figure 1), an *N*-heterocyclic polynuclear aromatic compound (NPA), is found in a variety of environmentally prevalent complex mixtures (1–3). The compound has been shown to be one of the most active carcinogens among NPAs and most of the polycyclic aromatic hydrocarbons (PAH) (4–7). In the hamster model for human bronchiogenic carcinoma, DBC demonstrated a higher tumorigenic activity than benzo[a]pyrene (BaP) when equal quantities were administered in hematite (8,9). Recent work in this laboratory (10) has shown DBC to be as potent as BaP in mouse skin carcinogenesis, producing tumors in 48 of 50 mice within 36.6 weeks compared to the production of tumors in 48 of 50 mice in 32.4 weeks for BaP.

Investigations in our laboratory (11) and elsewhere (12) suggest that the metabolism of DBC is not strictly analogous to PAH or related NPA. For example, an *N*-hydroxylated metabolite of DBC has been identified (11), while benzacridines have been shown to form *N*-oxides (13). Perin *et al.* (12) identified mostly phenols as metabolites and further characterized 5-hydroxy-DBC and 3-OH-DBC as the major products. Traces of 2-OH-, 4-OH- and 6-hydroxy-7H-DBC, as well as a small quantity of one dihydrodiol, tentatively identified as the 3,4-dihydro-3,4-dihydroxy derivative of DBC, were also isolated. The observation that phenol metabolites make up a larger proportion of the total metabolites of DBC when compared to certain members of the benzacridine series was also discussed by Gill *et al.* (14) in their examination of 7-methyl-benzacridine metabolism. They observed that the proportion of dihydrodiol metabolites was dependent on the hydrocarbon structure.

It is reasonable to postulate that the biologic activity of DBC may be related to the pyrryl nitrogen, since isosters bearing sulphur, oxygen or carbon in place of the nitrogen demonstrate no carcinogenic activity (15). *N*-alkylation has been shown to alter the *in vivo* carcinogenic profile. Kirby and Peacock have demonstrated that *N*-methyl-DBC induces local sarcomas, rather than liver tumors observed for the parent compound (16). The parent compound was also more hepatotoxic. Recent studies by Parks *et al.* (17) showed that DBC was more effective at producing mutations and adducts than the *N*-methyl derivative, and was more cytotoxic *in vitro*. Schurdak *et al.* (18) compared the abilities of DBC and *N*-methyl-DBC to form adducts in skin

*Abbreviations: DBC, 7H-dibenzo[c,g]carbazole; 2-OH-DBC, 2-hydroxy-7H-dibenzo[c,g]carbazole; 3-OH-DBC, 3-hydroxy-7H-dibenzo[c,g]carbazole; 4-OH-DBC, 4-hydroxy-7H-dibenzo[c,g]carbazole; 13c-OH-DBC, 13c-hydroxy-dibenzo[c,g]carbazole; *N*-methyl-DBC, *N*-methyl-dibenzo[c,g]carbazole; NPA, *N*-heterocyclic polynuclear aromatics; PAH, polycyclic aromatic hydrocarbons; BaP, benzo[a]pyrene. Hepes, hydroxyethylpiperidine sulfonic acid; HBSS, Hanks basic salt solution; RLC, rat liver cells; DMSO, dimethylsulfoxide; HGPRT, hypoxanthine–quanine phosphoribosyl transferase; FBS, fetal bovine serum; DMEM, Dulbecco's modified Eagle's medium; 3-MC, 3-methylcholanthrene; TMS, tetramethylsilane.

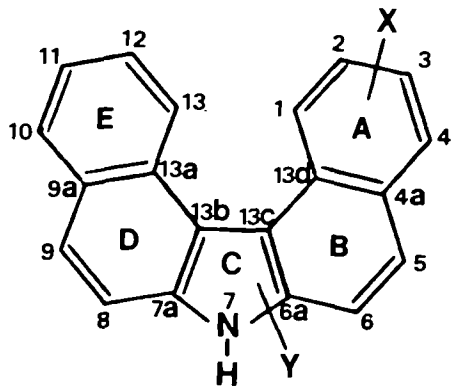

Fig. 1. Structure and labeling conventions of derivatives of DBC.

Compound	*X*	*Y*
DBC	H	H
2-OH-DBC	2-hydroxy	H
3-OH-DBC	3-hydroxy	H
4-OH-DBC	4-hydroxy	H
13c-OH-DBC	H	13c-hydroxy
N-methyl-DBC	H	N-methyl

and liver following topical application in mice. The findings indicated that DBC and the *N*-methyl derivative show marked organ specificity toward both adduction levels and adduct patterns in liver and skin.

We have undertaken the task to identify the metabolic pathways by which DBC is converted to its active intermediates. Schoeny and Warshawsky (19) have shown that mutagenicity of DBC to *Salmonella typhimurium* in a forward mutation assay is dependent on the presence and type of S-9 fraction used. Examination of the mutagenicity of metabolites indicated that the activity of 2-OH-, 4-OH- and 3-OH-DBC increased in that order. DBC was not active in a reverse mutation assay. *In vitro* binding of DBC to calf thymus DNA, RNA or polynucleotides (20) showed that, in the presence of rat liver microsomes, DBC bound preferentially to polyguanylic acid, although to a lesser extent than BaP. Schurdak *et al.* (21) demonstrated that 3-OH-DBC, a potential proximate genotoxicant, is capable of binding to mouse liver DNA by a ^{32}P-postlabeling technique, and that treatment with DBC produces similar adduct patterns, implying that oxidation at C3 is involved in the activation of the compound.

It is apparent that the appearance and activity of phenolic metabolites and derivatives of DBC are important in the investigation of the activation of the compound. Previous investigations into the process have been hampered by instability of synthetic standards of DBC derivatives (12). In this paper we report both the synthesis and complete characterization of stabile standards necessary in support of previously published work (11,18–21) and present investigations into the metabolism and activation of DBC.

Materials and methods

Chemicals

Unlabeled BaP was obtained from Aldrich Chemical Company (Milwaukee, WI) and recrystallized from benzene–isopropanol. [7,10-^{14}C]BaP (21 mCi/mmol) and (1,4,5,9,10,13,13b,13c–^{14}C]DBC (2.7 mCi/mmol) were obtained from Amersham (Arlington Heights, IL). All radiolabeled materials were checked for purity before use by HPLC (11).

DBC and its phenolic derivatives were prepared by using the Fischer indole synthesis (22) as adapted by Buu-Hoi *et al.* (23) and Perin *et al.* (12) with specific modifications. 5-, 6- and 7-methoxy-β-tetralone were substituted for the β-tetralone used to obtain the parent compound to synthesize 2-OH-, 3-OH- and 4-OH-DBC, respectively. Modifications involved the use of 2,3-dichloro-5,6-dicyano-1,4-benzoquinone to ring aromatize the 5,6-dihydro-methoxy-DBC isomers to their respective methoxy-DBC derivatives and the use of boron tribromide as a demethylation agent, as described by Fieser and Fieser (24,25), to convert the methoxy-DBC to their corresponding stable phenols. The synthesis of 13c-OH-DBC was achieved by refluxing DBC with benzoyl peroxide in dichloromethane for five days. *N*-methyl-DBC was obtained by *N*-alkylation of DBC using the method of Stevens and Tucker (26). All compounds were purified by thick layer chromatography using dichloromethane as the developing solvent and recrystallization from acetone–water to >99% pure as determined by HPLC techniques.

Collagenase (Type IV) was purchased from Sigma Chemical Co. (St. Louis, MO). Calcium- and magnesium-free Hank's Basic Salt Solution at pH 7.40 was used for collagenase solutions. Chemicals used in the preparation were obtained from Fisher Chemical Company (Cincinnati, OH) with the exception of hydroxyethylpiperidine sulfonic acid (Hepes) (Research Organics, Inc., Cleveland, OH). Culture media, fetal bovine serum (FBS), Hank's Basic Salt Solution (HBSS) and trypsin solution were obtained from Gibco Laboratories (Grand Island, NY). Luciferin–luciferase and ATP standard (disodium salt) (ATP assays) and diphenylamine used in the determination of DNA were obtained from Sigma Chemical Co. (St Louis, MO).

Analytical procedures

Metabolite samples dissolved in chloroform were chromatographed on a Varian 8500 HPLC unit fitted with a 25 × 4.8 mm, 10 μm particle size Whatman Partisil-10 ODS-2 reversed-phase column. A methanol–water gradient (76–100% methanol) with a flow of 1 ml/min was used and the effluent was monitored at 268 nm. Fractions corresponding to HPLC peaks for microsomal incubations or 0.5 ml fractions for rat hepatocyte incubations were collected and the radioactivity quantified by scintillation spectrometry (11).

Mass spectral data were collected using a Kratos model MS80 high performance mass spectrometer and continually processed with a Data General Nova/4C DS-55 data system. High resolution analyses were conducted by the direct probe method using an internal standard of perfluorokerosine within the source temperature at 200°C, and the probe temperature increased at 3°C/s. Fragments in the mass range of 70–355 a.m.u. were monitored using a 35 eV impact energy with a resolution of 3000.

NMR spectra were obtained using a Nicolet model NT-300, 300 MHz narrow bore spectrometer in solutions of deuterated chloroform with chemical shifts reported in p.p.m. relative to tetramethylsilane (TMS). Radioactivity of samples was determined using a Packard Model 3755 liquid scintillation spectrometer. Counting efficiencies of the samples were determined using [^{14}C]toluene as an internal standard. IR spectra of compounds in chloroform solution were obtained using a Perkin-Elmer model 599 IR Spectrophotometer. UV and corrected fluorescence spectra were obtained for compounds in ethanol solutions using a Beckman DB-GT grating UV spectrophotometer and a Corrected American Instrument Co. spectrophotofluorometer, respectively. Yellow lighting was used to minimize photo-oxidation during the experimental procedures.

Metabolism studies

Rat liver microsomal preparations were performed as previously described (11). Labeled or unlabeled DBC was added as an ethanol solution, and incubated for 60 min. The reaction was quenched with ice-cold acetone and the aqueous suspension was extracted twice with 4 ml ethyl acetate which was evaporated to dryness under N_2 at 40°C until further analysis.

Suspensions of rat liver cells (RLC) were isolated from male Sprague–Dawley rats (150–225 g) by the procedure of Seglen (27) as adapted for this laboratory. Calcium- and magnesium-free HBSS (25 mM Hepes, pH 7.4) was used as the perfusate followed by a solution of 180 mg collagenase in 150 ml of calcium- and magnesium-free HBSS. All solutions were continuously bubbled with compressed air. The cell suspension was purified by centrifugation, and cells were counted using a Coulter Counter. Cells (5×10^6) were plated in 9 ml of William's Media E plus 1 ml FBS. Cell viability was determined by Trypan Blue exclusion for cell suspensions and by ATP content for 24 h cultures using the procedure of Holm-Hansen *et al.* (28). DNA content of RLC cultures were determined using the method of Burton (29). Cultures were incubated at 37°C in a humidified 95% air/5% CO_2 atmosphere.

For identification of DBC metabolites in RLC 4.33 μCi of [^{14}C]DBC in dimethylsulfoxide (DMSO) was added to a final concentration of 50 μM DBC and incubated for 24 h. Medium and cell washes (2 × HBSS) were extracted three times with 25 ml ethyl acetate. Aliquots of the extracted aqueous layer and the ethyl acetate layer were used to determine the level of non-extractable metabolites and extractable metabolites, respectively. The remainder of the ethyl acetate layer was evaporated to dryness under N_2 at 40°C. The residue was stored at −20°C for HPLC analysis.

Metabolism of BaP and DBC in RLC cultures was determined by the procedure of DePierre *et al.* (30) as modified by VanCantfort *et al.* (31) and adapted for

use in RLC cultures in this laboratory. For comparative metabolism studies 5×10^6 cells/flask were incubated undisturbed overnight followed by media replacement without FBS. Acetone solutions of either [^{14}C]DBC or [^{14}C]BaP were added to achieve final concentrations of 10, 25, 50 or 100 μM substrate, respectively. At zero, 0.5, 1.0 and 2.0 h, 1 ml aliquots were removed, mixed immediately with 1 ml of 0.15 M KOH in 85% DMSO, the parent compound was extracted with hexane, and radioactivity of the aqueous layers was quantified. Metabolites and compounds more polar than DBC were found only in the ethyl acetate extracts while only DBC was found in the hexane extract. To correct for the DBC remaining in the aqueous layer after the hexane extraction, experiments were carried out utilizing cultures fixed with acetic acid and rinsed and media alone without cells. Values of control determinations were subtracted from raw data and adjusted for changes in volume of media from sampling to obtain final metabolism results.

RLC/DPI-3 mutagenesis assay

Mutagenic activities of BaP, DBC and DBC derivatives were determined in a co-cultivation system utilizing RLC as the metabolizing layer and DPI-3 cells, an epithelial line derived from embryonic hamster (32), as the marker layer. The mutation at the hypoxanthine-guanine phosphoribosyl transferase (HGPRT) locus was determined by resistance to 6-thioguanine toxicity as characterized by Dooley in this laboratory (33).

Co-cultivation procedures were initiated by plating 1×10^6 DPI-3 cells into 75 cm^2 sterile tissue culture flasks in 9 ml of Dulbecco's Modified Eagle's medium (DMEM) and 1 ml FBS. After 24 h, the medium was aspirated and 3×10^6 RLC were plated in 9 ml of William's Media E and 1 ml FBS. After an additional 24 h, cells were re-fed with 9 ml of William's Media E and 1 ml FBS and DMSO alone or individual compounds in DMSO to achieve a final concentration of 40 μM. Untreated controls were also conducted. Following a 48 h exposure period, cells were allowed to recover for 40 h in 9 ml of DMEM plus 1 ml FBS, and then were subcultured in the same medium every two days. After five passages, mutant colonies were screened in DMEM/10% FBS containing 60 μM 6-thioguanine and the plating efficiencies were determined in DMEM/10% FBS. After 5–6 days of incubation, cells were rinsed with isotonic saline, fixed with ethanol and stained with Trypan Blue for counting viable colonies. The mutation frequency was determined as the ratio of viable mutant colonies to total viable colonies (five determinations from each treatment flask), and was expressed as mutants per 10^5 survivors. Each compound was tested in duplicate flasks for each of two independent experiments utilizing an individual RLC isolation and co-cultivation procedure except for *N*-methyl-DBC, which was tested in duplicate for one experiment only. The numbers reported for mutagenic response represent the average of the four determinations.

Statistical procedures

Significant differences between rates of metabolism and mutagenic responses for DBC and BaP were determined using the Student's *t*-test at each concentration ($P = 0.05$). Analysis of variance procedures were used to determine significant differences in mutagenic responses of DBC and its derivatives ($P = 0.05$). Mutagenic responses were first transformed to achieve normal distribution using the method described by Snee and Irr (34). The method utilizes a power transformation of the form:

$Y = (X + A)^{\lambda}$, where X is the mutagenic response, $A = 1$ and $\lambda = 0.15$. Values for A and λ were established in our laboratory using historical data for DPI-3 mutagenesis (35).

Animals

Male Sprague–Dawley rats were purchased from Charles River Laboratories (Kingston, NY), housed in stainless steel cages under a 12 h day/night cycle and allowed free access to standard laboratory chow and water. Animals were allowed a 2 week period for adjustment to the surroundings prior to use.

Results

Synthetic standards

The purity of compounds obtained through synthetic procedures were assessed by HPLC analyses of solutions in dichloromethane or chloroform. Compound purity was estimated by the ratio of product peak height to the total of observed peak heights. Purity was >99% for all compounds. Phenols isolated using the stated synthetic procedure were found to be stable under subdued lighting in air either in dichloromethane solution or as solids.

Derivatives were analyzed by high resolution mass spectrometry (Table I) and NMR (Table II). Complete UV and fluorescence spectra are presented in Table III, along with IR spectra for 13c-OH-DBC and DBC. Observed melting points (uncorrected) and yields after purification for DBC and derivatives were as follows: DBC: 210°C, 62%; 2-OH-DBC: 110–120° (decomposition), 25%, 3-OH-DBC: 110–120° (decomposition), 12%; 4-OH-DBC: 184°C, 25%; 13c-OH-DBC: 110–120° (decomposition), 19%; *N*-methyl-DBC: 122°C, 90%.

DBC metabolite identification

The HPLC profile of the synthetic standards of DBC is shown in Figure 2A, and the metabolite profile from 3-MC-induced microsomal incubations is shown in Figure 2B. The microsomal metabolite profile differs only slightly from that originally published (11) due to changes in incubation and analysis techniques. Fractions corresponding to the numbered peaks from unlabeled substrate incubations were collected and analyzed by high resolution mass spectrometry for metabolite identification. Results of high resolution mass spectral analyses indicated that peaks 2, 3, 3b, 4 and 5 all contained phenol isomers of DBC. Peak 1 contained radiolabel, but no DBC-derived fragment could be identified. Peak 7 was found to contain a fragment with the same *m/e* as the parent compound (267 a.m.u.).

Positive identification of metabolites of the ethyl acetate extracts of the microsomal preparation was accomplished by UV, fluorescence and mass spectral techniques, and cochromatography with the synthetic standards (see Figure 2, Tables I–III). 2-OH-DBC and 3-OH-DBC were positively identified as metabolites in the extract, at retention times of 8 and 10 min, respectively. The mass spectral analyses of these two metabolites gave a *m/e* of 283.1037 and 283.1023 for the 2-OH- and 3-OH-DBC, respectively, with an elemental analysis of $C_{20}H_{13}NO$. The UV and fluorescence spectra produced peaks that were coincident with those of the synthetic standards described in Table III. 4-OH-DBC eluted at 12 min and did not correspond to any of the peak assignments in extracts. Similarly, *N*-methyl-DBC and 13c-OH-DBC were not identified as metabolites. 13c-OH-DBC eluted at 16 min, and the less polar *N*-methyl-DBC eluted after the parent compound at 28 min. Although *N*-methyl-DBC had a retention time between peaks 8 and 9, it co-chromatographed with neither peak.

In RLC cultures treated with 50 μM [^{14}C]DBC, 27.6% was found in the cells, 44.7% in the ethyl acetate extract of the media and 27.6% in the extracted media. Total recovery was 107%. The ethyl acetate extract was analyzed by HPLC and representative results are shown in Figure 2C. Of the radiolabel, 67% represented the parent compound but the metabolite profile had notable differences from that seen in the microsomal studies (Figure 2B). Peaks with retention times of 2-OH- and 3-OH-DBC were present, but peaks corresponding to 4-OH-DBC, 13c-OH-DBC or *N*-methyl-DBC were not found. In addition, radiolabel in peak 4 was small in the RLC profile (Figure 2C) in relation to the absorbance peak in the microsomal profile (Figure 2B).

The percent of total metabolism of DBC in corn oil and 3-MC-induced microsomal preparations was 20 and 38%, respectively. Fractions corresponding to the numbered peaks in Figure 2B were compared to metabolite quantities observed in RLC extractions (Table IV). Quantities are expressed as percent of total observed metabolites. RLC extracts generally demonstrate greater amounts of polar compounds (shorter retention times) and lower amounts of the less polar compounds (longer retention times) relative to the corn oil microsomal extracts. Incubation with 3-MC-induced microsomes resulted in an increase in the total observed metabolites, a large relative increase in the amount of peak 4 (22.7% versus 5.5% and 8.2%), and a decrease in the amounts of peaks 7, 8 and 9, compared to the incubations with corn oil control microsomes. Decomposition of peak 4 metabolite from

Table I. Mass spectral data of 7H-dibenzo[*c,g*]carbazole standards

Compound	Molecular ion			Major fragments		
	observed mass (expected)	relative intensity	elemental analysis	mass	relative intensity	elemental analysis
DBC	267.1034 (267.1048)	100.00	$C_{20}H_{13}N$	—	—	—
2-OH-DBC	283.0964 (283.0997)	100.00	$C_{20}H_{13}NO$	267.1049	13.39	$C_{20}H_{13}N$
				255.1043	1.49	$C_{19}H_{13}N$
				254.0967	7.25	$C_{19}H_{12}N$
3-OH-DBC	283.0971 (283.0997)	100.00	$C_{20}H_{13}NO$	267.1032	2.05	$C_{20}H_{13}N$
				254.0983	11.40	$C_{19}H_{12}N$
				252.0833	11.01	$C_{19}H_{10}N$
4-OH-DBC	283.1008 (283.0997)	100.00	$C_{20}H_{13}NO$	267.1048	1.10	$C_{20}H_{13}N$
				254.0957	25.52	$C_{19}H_{12}N$
13c-OH-DBC	283.0926 (283.0997)	1.92	$C_{20}H_{13}NO$	282.0888	0.91	$C_{20}H_{12}NO$
				267.1108	100.00	$C_{20}H_{13}N$
N-methyl-DBC	281.1209 (281.1205)	100.00	$C_{21}H_{15}N$	265.0885	22.67	$C_{20}H_{11}N$

Table II. NMR spectral data of synthetic 7H-dibenzo[*c,g*]carbazole standards[a]

Compound	Spectra
DBC	H_1 = 9.22 (d) H_2 = 7.69 (dd) H_3 = 7.52 (dd) H_4 = 8.04 (d) H_5 = 7.70 (d) H_6 = 7.88 (d) H_7 = 8.78 (s) $J_{1,2}$ = 8.4 $J_{2,3}$ = 6.8 $J_{3,4}$ = 8.1 $J_{5,6}$ = 8.7
2-OH-DBC	H_1 = 8.55 (s) H_3 = 7.5 (d) H_4 = 7.93 (d) H_5 = 7.66 (d) H_6 = 7.80 (d) H_7 = 8.75 (s) H_8 = 7.86 (d) H_9 = 7.66 (d) H_{10} = 8.04 (d) H_{11} = 7.50 (dd) H_{12} = 7.69 (dd) H_{13} = 9.14 (d) $J_{3,4}$ = 8.04 $J_{5,6}$ = 8.6 $J_{8,9}$ = 8.7 $J_{10,11}$ = 8.1 $J_{11,12}$ = 8.8 $J_{12,13}$ = 8.4
3-OH-DBC	H_1 = 9.15 (d) H_2 = 7.67 (d) H_4 = 7.40 (s) H_5 = 7.71 (d) H_6 = 7.74 (d) H_7 = 8.75 (s) H_8 = 7.87 (d) H_9 = 7.71 (d) H_{10} = 8.08 H_{11} = 7.51 (dd) H_{12} = 7.49 (dd) H_{13} = 9.13 (d) $J_{1,2}$ = 7.2 $J_{5,6}$ = 8.7 $J_{8,9}$ = 8.7 $J_{10,11}$ = 8.1 $J_{11,12}$ = 7.2 $J_{12,13}$ = 7.2
4-OH-DBC	H_1 = 8.81 (d) H_2 = 7.53 (dd) H_3 = 6.89 (d) H_5 = 8.34 (d) H_6 = 7.70 (d) H_7 = 8.78 (s) H_8 = 7.89 (d) H_9 = 7.70 (d) H_{10} = 8.04 (d) H_{11} = 7.70 (dd) H_{12} = 7.52 (dd) H_{13} = 9.21 (d) $J_{1,2}$ = 8.1 $J_{2,3}$ = 7.5 $J_{5,6}$ = 8.7 $J_{8,9}$ = 8.7 $J_{10,11}$ = 7.8 $J_{11,12}$ = 8.1 $J_{12,13}$ = 8.4
N-methyl-DBC[b]	H_1 = 9.14 (d) H_2 = 7.62 (dd) H_3 = 7.45 (dd) H_4 = 7.98 (d) H_5 = 7.67 (d) H_6 = 7.87 (d) $J_{1,2}$ = 8.7 $J_{2,3}$ = 7.2 $J_{3,4}$ = 7.8 $J_{5,6}$ = 9.0
13c-OH-DBC	H_1 = 7.92 (d) H_2 = 7.35 (dd) H_3 = 7.10 (d) H_4 = 7.26 (d) H_5 = 6.87 H_6 = 6.71 (d) H_8 = 7.87 (d) H_9 = 7.55 (d) H_{10} = 7.96 (d) H_{11} = 7.42 (dd) H_{12} = 7.50 (dd) H_{13} = 8.16 (d) $J_{1,2}$ = 7.2 $J_{2,3}$ = 7.5 $J_{3,4}$ = 5.4 $J_{5,6}$ = 9.0 $J_{8,9}$ = 8.3 $J_{10,11}$ = 8.7 $J_{11,12}$ = 7.1 $J_{12,13}$ = 8.4

[a]All chemical shifts were determined in $CDCl_3$ solution with respect to tetramethylsilane.
[b]The sequence of *N*-methyl-DBC also contains a singlet integrating for three hydrogens at δ = 4.05.

3-MC-induced microsomal extractions was observed with time with a corresponding increase in peaks 5, 8 and 9 of which 8 is the largest. Peak 5, which does not correspond to any peaks in the profile reported by Perin *et al.* (12), decomposed similarly in our system to peaks 8 and 9.

Metabolism of DBC in RLC

Rate of DBC metabolism was determined by the appearance of total metabolites over a 2-h period using a range of substrate concentrations (Figure 3A). Appearance of DBC metabolites was observed to be concentration dependent over the concentration

Table III. Fluorescence and IR spectral data for 7H-dibenzo[c,g]carbazole standards

Compound	Spectra
DBC	UV (nm): 223, 230 (s), 240, 252 (s), 277, 299, 332, 347, 364 IR (cm^{-1}) (KBr): 3450, 3050, 1600, 1375, 1325, 800, 710 Fluorescence (nm) Excitation: 223, 240 (s), 277 (s), 300, 330 (s), 347, 369 Emission: 371, 389, 410 (s), 435 (s)
2-OH-DBC	UV (nm): 223, 230 (s), 240, 252 (s), 277, 299, 332, 347, 364 359 (s), 364 Fluorescence (nm) Excitation: 222, 235 (s), 280, 307 (s), 350, 364 Emission: 377, 392, 413 (s)
3-OH-DBC	UV (nm); 247, 277, 302, 334 (s), 348, 363, 375 (s) Fluorescence (nm): Excitation: 223, 277, 304, 354 (s), 366, 377 (s) Emission: 397, 412
4-OH-DBC	UV (nm): 220, 232, 249, 279, 300 (s), 338 (s), 354, 371 Fluorescence (nm): Excitation: 222, 282, 300 (s), 340 (s), 358, 374 Emission: 385, 402, 425 (s)
13c-OH-DBC	UV (nm): 225, 237, 267, 280, 300 (s), 345, 367 IR (cm^{-1}) (KBr): 2950, 2750, 1725, 1452, 1250, 1100, 1000, 800, 710 Fluorescence (nm): Excitation: 220, 230 (s), 277, 300 (s), 330 (s), 352, 369 Emission: 372, 392, 410 (s)
N-methyl-DBC	UV (nm): 222, 230 (s), 240, 256, 280, 303, 337 (s), 348, 367 Fluorescence (nm): Excitation: 223 (s), 237, 282, 304, 340 (s), 353, 370 Emission: 377, 397, 420 (s), 447 (s)

(s) = shoulder.

range tested and linear from 0.5 to 2 h. Similar to DBC, the appearance of BaP metabolites was concentration dependent over the range tested and was linear over a comparable time course (Figure 3B). However, fewer BaP metabolites were observed at each time point and substrate concentration in comparison to DBC. The rates are presented for comparative purposes in Figure 3C. At substrate concentrations of 10 and 25 μM, rates of appearance of metabolites for the two compounds are equivalent. At high substrate concentrations of 50 and 100 μM, however, the rates of appearance of DBC metabolites are significantly greater than those of BaP. BaP metabolism reaches an apparent saturation at ~25 μM substrate concentration, while DBC rates increase in proportion to concentration throughout the concentration range tested. At 100 μM, DBC metabolites appear in the medium ~4-times faster than those of BaP.

Comparative mutagenesis of DBC and BaP

Co-cultivations of RLC and DPI-3 cells were treated with either BaP or DBC in DMSO at concentrations of 0.4, 4.0 and 40.0 μM in order to directly compare the potency of the two compounds (Figure 4). Controls consisted of cultures with and without DMSO. Each point represents the average of duplicate determinations. The average mutation frequencies observed for untreated controls and DMSO controls were 1.05 ± 0.36 (SD) and 0.17 ± 0.24 mutants/10^5 survivors, respectively. Mutagenic response was found to be linear to log doses of DBC over the concentrations range tested. In contrast, mutagenic responses to BaP were shown to be curvilinear to long doses. Furthermore, mutant frequencies for DBC were higher than those observed for BaP at each concentration tested. Statistical procedures indicate that the mutation frequencies of BaP and DBC were significantly different ($P < 0.01$) at all concentrations tested.

Mutagenesis of DBC and derivatives

2-OH and 3-OH-DBC, identified as metabolites in both microsomal and RLC incubations, as well as 4-OH, 13c-OH and *N*-methyl-DBC, which were not identified as metabolites, were compared to the parent compound for mutagenic activity in the RLC/DPI-3 whole-cell co-cultivation system (Table V). The parent compound was found to induce 8.0 ± 2.8 mutants/10^5 survivors. *N*-methyl-DBC and 13c-OH were as potent as the parent compound, including 12.9 ± 5.4 and 8.0 ± 3.1 mutants/10^5 survivors, respectively. Of the three phenols tested, only 3-OH was found to be mutagenic, inducing 4.4 ± 0.8 mutants/10^5 survivors. 4-OH-DBC was not found to be mutagenic at 0.4, 4 or 40 μM (data not shown).

Discussion

The synthesis of stable DBC derivatives has allowed us to investigate their mutagenesis in bacterial systems (19), DNA binding *in vitro* (20) and *in vivo* (18,21), and the metabolism and mutagenesis in mammalian whole-cell systems. By utilizing boron tribromide for cleavage of the methoxy DBC derivatives to stable phenols, we have been able to provide a more detailed characterization of many of the metabolites and several related derivatives using UV, IR, fluorescence spectroscopy, high resolution NMR and mass spectrometry.

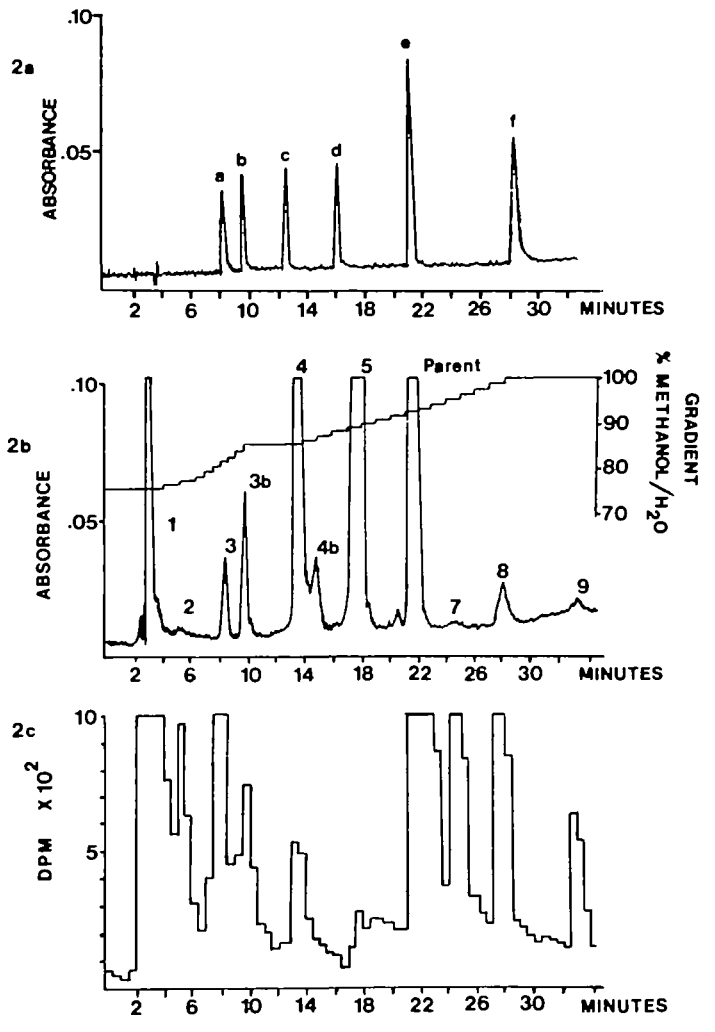

Fig. 2. Reversed-phase HPLC separation of DBC metabolites isolated from incubations of DBC with 3-MC-induced rat liver microsomes or with control rat liver cell cultures. (A) Chromatogram of DBC derivative standards. Peak a, 2-OH-DBC; peak b, 3-OH-DBC; peak c, 4-OH-DBC; peak d, 13c-OH-DBC; peak e, DBC; peak f, *N*-methyl-DBC. Standards are detected by UV absorbance at 268 nm. (B) Chromatogram of metabolites isolated by ethyl acetate extraction from 3-MC induced liver microsomes incubated with DBC. Peak 3, 2-OH-DBC; peak 3b, 3-OH-DBC; peaks 2, 4 and 5 are unidentified DBC phenols. Other numbered peaks are unidentified DBC-related products. Metabolites are detected by UV absorbance at 268 nm. (C) Chromatogram of metabolites isolated by ethyl acetate extraction from the medium of cultured rat liver cells incubated with 50 μM [^{14}C]DBC. Metabolites are detected by liquid scintillation spectrometry of 0.5 ml collections of effluent.

Our results indicate that phenols are the predominate metabolites of DBC. This observation is in contrast to those for members of the benzacridine series which demonstrate a much higher proportion of dihydrodiol and catechol metabolites (13,14,36–38). Phenols are formed either by intramolecular rearrangement of epoxides (38) or through direct hydroxylation of a specific position in the molecule (39). The formation of dihydrodiols or catechols relies on epoxides stable enough to undergo enzymatic hydration or bimolecular reactions with water. The observation that phenols are the predominate metabolites of DBC implies that either the intermediates undergo intramolecular rearrangement more readily than PAH or related NPA, or that oxidation is exclusively by direct hydroxylation. If either mechanism operates, the compound is not strictly analogous to

Table IV. Quantitation of metabolites in rat liver microsomal and rat liver cell incubations

HPLC peak[b]	Percent of total metabolites[a]		
	corn oil control liver microsomes	3-MC induced liver microsomes	cultures of liver cells
1	3.5 ± 0.1	3.6 ± 3.3	7.3 ± 1.1
2	3.4 ± 0.2	2.6 ± 0.1	12.6 ± 4.9
3	10.3 ± 0.8	10.5 ± 0.5	14.2 ± 1.7
3b	4.5 ± 0.4	5.3 ± 0.0	9.6 ± 0.2
4	5.5 ± 0.3	22.7 ± 1.8	8.2 ± 0.9
4b	3.8 ± 0.7	5.1 ± 0.1	3.1 ± 0.7
5	5.2 ± 0.5	5.7 ± 0.7	5.7 ± 1.6
7	21.0 ± 0.3	10.7 ± 1.2	14.0 ± 3.6
8	24.7 ± 1.1	18.6 ± 1.6	16.5 ± 4.1
9	18.2 ± 0.9	15.2 ± 0.5	8.6 ± 2.4

[a]Percent as averages of duplicate determinations ± SD.
[b]Peak numbers correspond to those shown in Figure 2B.

PAH or to other NPA. Such reactions would be consistent with the high reactivity of DBC intermediates based on its observed carcinogenic activity.

We identified 2-OH- and 3-OH-DBC as metabolites in whole cell and microsomal systems. 4-OH-DBC was not found in either system. Perin *et al.* (12) identified 2-OH- and 3-OH-DBC, and also reported 4-OH-, 5-hydroxy- and 6-hydroxy-DBC as metabolites in microsomal incubations. Although we did not have standards for the 5-hydroxy- and 6-hydroxy-DBC, we observed several phenol metabolites that were not positively identified in our system. Peak 4 (Figure 2) could correspond to the 5-hydroxy-DBC isomer, based on its high levels in the extracts of 3-MC-induced microsome incubations, and on the observation that the peak disappeared with time with a concomitant increase in peak 8. Perin *et al.* (12) made a similar observation, characterizing the phenomenon as dimerization of 5-hydroxy-DBC to 6,6'-bis-DBC. On the other hand, we have not been able to characterize our peak 8 as a dimerization product of 5-hydroxy-DBC. Rather, peak 8 appears to be a dimer of a compound with a mol. wt of 310, a catechol of DBC. In addition, Perin *et al.* (12) identified 3,4-dihydroxy-3,4-dihydro-DBC as a metabolite. Although we have no dihydrodiol standards available, mass spectral analyses of the isolated metabolite fractions did not indicate the presence of dihydrodiols. Peak 5 in our system was not observed by Perin *et al.* (12).

We observed an important difference in metabolite profiles between incubations with 3-MC-induced microsomes and incubations with corn oil control microsomes and RLC. Peak 4, a major product of 3-MC-induced microsomal incubations, is much lower in extracts of both control preparations (Table IV). 3-MC-induced microsomes appear to increase levels of oxidation of DBC at that position.

Insight into the basis for the high carcinogenic activity of DBC can be gained by comparison of the rates of metabolism and mutagenesis for BaP and DBC (Figure 3). The rates for DBC metabolism, as measured by appearance of metabolites in the medium, were higher than those for BaP at 50 μM and above, implying the DBC is metabolized at a faster rate than BaP. At lower concentrations, which are more likely to be comparable to physiological concentrations, the rates are statistically indistinguishable. However, at all concentrations tested for mutagenesis where the rates of metabolism were comparable (<25 μM substrate), DBC was found to be significantly more

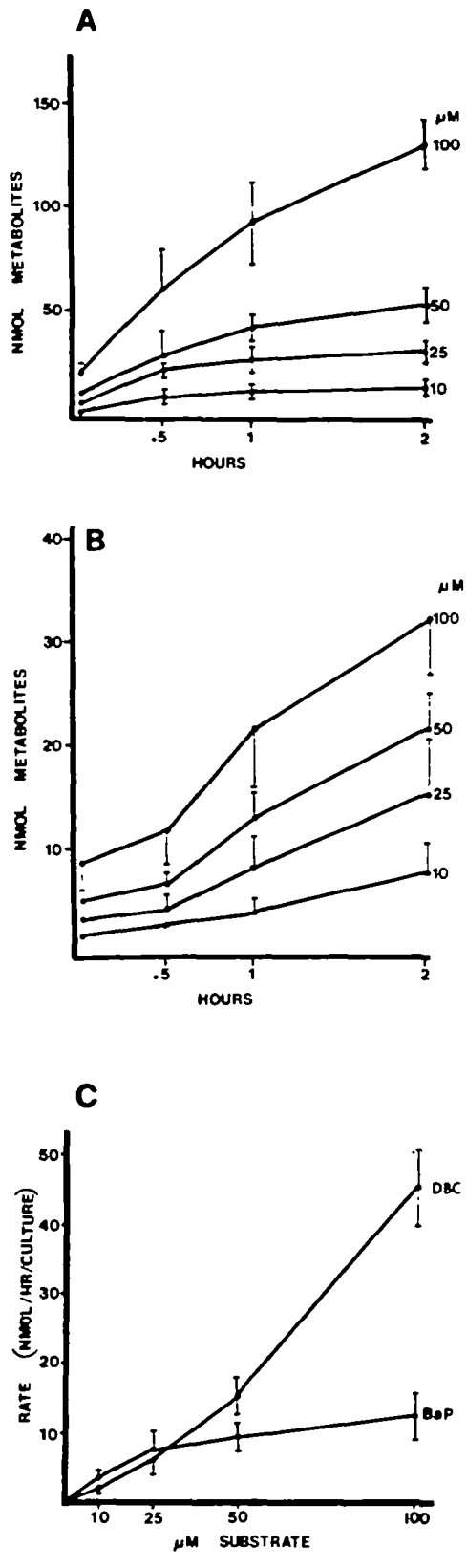

Fig. 3. Time course of appearance of metabolites of (A) DBC and (B) BaP in the medium of cultured RLC incubated with 10, 25, 50 or 100 μM substrate. Each curve represents the average of four individual RLC incubations. (C) Rates of metabolism of DBC and BaP for each of the four substrate concentrations. The rates were calculated as the slope of time course curves (A) and (B) by linear regression techniques, using the time points from 0.5 to 2.0 h.

Table V. Mutation frequencies for 7H-dibenzo[c,g]carbazole and derivatives of DPI-3 cells

Compound	Mutant colonies[a]	Plating efficiency (%)	Mutants/10^5 survivors[a]
DMSO	0.7 ± 0.1	78.6	1.0 ± 0.2
DBC	6.2 ± 1.8	87.9	8.0 ± 2.8[b]
2-OH-DBC	1.4 ± 1.2	79.6	2.0 ± 1.6
3-OH-DBC	3.2 ± 0.6	79.4	4.4 ± 0.8[b]
4-OH-DBC	2.4 ± 0.9	90.1	2.9 ± 0.7
13c-OH-DBC	6.5 ± 2.6	91.4	8.0 ± 3.1[b]
N-methyl-DBC	8.9 ± 3.5	76.5	12.9 ± 5.4[b]

[a]Mean ± SD.
[b]Different from DMSO controls by analysis of variance procedures.

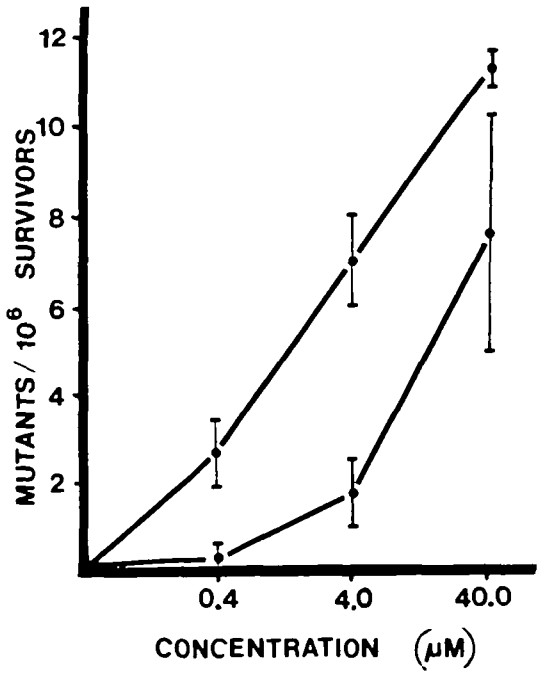

Fig. 4. Number of mutant (6-thioguanine resistant) colonies observed after incubation with 0.4, 4.0 and 40.0 μM DBC, or BaP in the RLC-DPI-3 cell co-cultivation system. Each point represents the average of four determinations. Mutation frequencies for untreated controls and solvent (DMSO) controls were 1.05 ± 0.36 and 0.17 ± 0.24 mutants/10^5 survivors, respectively.

mutagenic than BaP. These findings suggest that either DBC is more efficiently converted to active intermediate(s) than BaP, or that the active intermediate(s) is more efficient in its induction of mutations in this system.

The available phenol standards were tested for mutagenic activity in the whole cell co-cultivation system (Table V). Only 3-OH-DBC shows mutagenic activity and that is at a level below that observed for the parent compound. The implication that oxidation at C3 is involved in the activation of DBC is supported by post-labeling identification of adducts *in vivo* (18,21), where similar adduct patterns are formed following treatment with 3-OH-DBC and DBC. The 2-OH- and 4-OH-DBC were inactive as mutagens. The 3-OH isomer is the only phenol of the three tested which is inductively linked to the nitrogen; this suggests that nitrogen-linked inductive effects control the mutagenic activity of metabolites and may explain the activity of the 3-OH compound in all systems. Other derivatives involving the nitrogen

through inductive mechanisms, *N*-methyl- and 13c-OH-DBC, were as active as the parent, further supporting the involvement of nitrogen induction mechanisms in the activation of the compound. The 13c-OH-DBC is relatively unstable because the hydroxy derivative at an annular carbon both disrupts the aromaticity and destroys the planarity of the molecule. Nucleophilic attack at the nitrogen (or at positions inductively linked to the nitrogen), with concomitant loss of the hydroxyl moiety at the 13c-position, would have a large driving force, since the aromaticity and planarity would be restored. The 13c-OH-DBC was not found as a metabolite, so the high mutagenic activity can only be suggestive of DBC chemistry in biological systems.

N-Methylation neither blocks nor enhances the mutagenic activity of the compound in our system, suggesting that the shift of carcinogenic activity observed *in vivo* for the *N*-methyl compound may be due in part to a pharmacokinetic effect, relating the compound's activity to the metabolic activity of the cells to which the *N*-methyl compound is distributed (18) rather than an enzymatic effect (40). *N*-methylation does not alter the *in vitro* metabolism, except for the appearance of an *N*-hydroxymethyl derivative (41). No evidence for *N*-demethylation was observed in those studies, a conclusion that was based primarily on the observation that no parent compound could be isolated. Parks *et al.* (17) recently found that *N*-methyl-DBC is less readily converted into forms capable of covalent binding to DNA, but on the basis of equal frequencies of adduct formation, both compounds are mutagenically equipotent. The results of our studies also indicate similar mutagenic potencies for the two compounds.

Our results indicate that the metabolism of DBC leads predominantly to phenols, an observation that makes DBC unique in comparison to PAH and other NPA. The rate of metabolism of DBC by RLC at high substrate concentrations is greater than that for BaP, and at lower concentrations DBC is more efficient at producing mutations than BaP. Mutagenic activity of specific phenols that were identified as metabolites is associated only with the compounds related to the nitrogen by induction. Derivatives not identified as metabolites but still associated with the nitrogen by induction were also mutagenic, supporting the hypothesis that the nitrogen is involved in the compound's activation.

Acknowledgements

This paper is dedicated to the fond memory of Dr Robert T.Christian. The work was supported by HHS research grants OH1701-01 (NIOSH), CA23515 (NCI) and ES04203 (NIEHS) Fellowships from Gulf Oil and Union Carbide, and NIEHS Toxicology Training Grant ES 07073. NMR and mass spectra operating costs were supported by National Science Foundation grants CHE 8102974 and PCM 8219912, respectively. We would like to thank Dr Elwood Brooks of the University of Cincinnati, Department of Chemistry, for generating the high resolution NMR spectra.

References

1. Van Duuren,B.L., Bilbao,J.A. and Joseph,C.A. (1960) The carcinogenic nitrogen heterocycles in cigarette smoke condensates. *J. Natl. Cancer Inst.*, **25**, 53–61.
2. Schiller,J.E. (1977) Nitrogen compounds in coal derived liquid. *Anal. Chem.*, **49**, 2292–2294.
3. Blumer,M., Dorsey,T. and Sass,J. (1977) Azaarenes in recent marine sediments. *Science*, **195**, 283–285.
4. International Agency for Research on Cancer (IARC) (1983) *Monographs on the Evaluation of Carcinogenic Risk to Man: Certain Polycyclic Aromatic Hydrocarbons and Heterocyclic Compounds*. Lyon, France, vol. 3.
5. Boyland,E. and Brues,A.M. (1937) The carcinogenic action of dibenzcarbazoles. *Proc. Roy. Soc. London (B)*, **122**, 429–440.
6. Andervont,H.B. and Shimkin,M.B. (1940) Biological testing of carcinogens. II. Pulmonary-tumor-induction technique. *J. Natl. Cancer Inst.*, **1**, 225–239.
7. Andervont,H.B. and Edwards,J.E. (1941) Hepatic changes and subcutaneous and pulmonary tumors induced by subcutaneous injection of 3,4,5,6-dibenzcarbazole. *J. Natl. Cancer Inst.*, **2**, 129–149.
8. Sellakumar,A. and Shubik,P. (1972) Carcinogencity of 7H-dibenzo[*c,g*]carbazole in the respiratory tract of hamsters. *J. Natl. Cancer Inst.*, **48**, 1641–1644.
9. Saffiotti,U., Cefis,F. and Kolb,L.H. (1968) A method for the experimental induction of bronchiogenic carcinoma. *Cancer Res.*, **28**, 104–124.
10. Warshawsky,D. and Barkley,W. (1987) Comparative potencies of 7H-dibenzo[*c,g*]carbazole, dibenz[*a,j*]acridine and benzo[*a*]pyrene in mouse skin. *Cancer Lett.*, **37**, 337–344.
11. Warshawsky,D. and Myers,B.L. (1981) The metabolism of 7H-dibenzo[*c,g*]carbazole, an *N*-heterocyclic aromatic, in the isolated perfused lung. *Cancer Lett.*, **12**, 153–159.
12. Perin,F., DuFour,M., Mispelter,J., Ekert,B., Kunneke,C., Oesch,F. and Zajdela,F. (1981) Heterocyclic polycyclic aromatic hydrocarbon carcinogenesis: 7H-dibenzo[*c,g*]carbazole metabolism by microsomal enzymes from mouse and rat liver. *Chem.-Biol. Interact.*, **35**, 267–284.
13. Jacob,J., Schmoldt,A., Kohbrok,W., Raab,G. and Grimmer,G. (1982) On the metabolic activation of benz[*a*]acridine and benz[*c*]acridine by rat liver and lung microsomes. *Cancer Lett.*, **16**, 297–306.
14. Gill,J.H., Bonin,A.M., Podobna,E., Baker,R.S.U., Duke,C.C., Ryan,A.J. and Holder,G.M. (1986) 7-Methylbenz[*c*]acridine: Mutagenicity of some of its metabolites and derivatives, and the identification of some of its metabolites and derivatives, and the identification of trans-7-methylbenz[*c*]acridine-3,4-dihydrodiol as a microsomal metabolite. *Carcinogenesis*, **7**, 23–31.
15. Arcos,J.C. and Argus,M.E. (1974) *Chemical Induction of Cancer*. Academic Press, New York, Vol. IIA.
16. Kirby,A.H.M. and Peacock,P.R. (1946) The influence of methylation on the carcinogenic activity. I. *N*-methyl-3,4,5,6-dibenzcarbazole. *Proc. Roy. Soc. London (B)*, **122**, 179–189.
17. Parks,W.C., Schurdak,M.E., Randerath,K., Maher,V.M. and McCormick,J.J. (1986) Human cell-mediated cytotoxicity, mutagenicity, and DNA adduct information of 7H-dibenzo[*c,g*]carbazole and its *N*-methyl derivative in diploid human fibroblasts. *Cancer Res.*, **46**, 4706–4711.
18. Schurdak,M.E., Stong,D.B., Warshawsky,D. and Randerath,K. (1987) *N*-Methylation reduces the DNA-binding activity of 7H-dibenzo[*c,g*]carbazole ~300-fold in mouse liver but only ~2-fold in skin: possible correlation with carcinogenic activity. *Carcinogenesis*, **8**, 1405–1410.
19. Schoeny,R. and Warshawsky,D. (1987) Mutagenicity of 7H-dibenzo[*c,g*]carbazole and its metabolism in *Salmonella typhimurium*. *Mutat. Res.*, **188**, 275–286.
20. Lindquist,B., Stong,D.B. and Warshawsky,D. (1986) Binding of 7H-dibenzo[*c,g*]carbazole to nucleic acid *in vitro*. In *Proceedings of the 9th International Symposium on Polynuclear Aromatic Hydrocarbons*, Battelle, Columbus, OH, pp. 495–503.
21. Schurdak,M.E., Stong,D.B., Warshawsky,D. and Randerath,K. (1987) ^{32}P-Postlabeling analysis of DNA adduction in mice by the synthetic metabolites of the environmental carcinogen, 7H-dibenzo[*c,g*]carbazole: chromatographic evidence for 3-hydroxy-7H-dibenzo[*c,g*]carbazole being a proximate genotoxicant in liver but not in skin. *Carcinogenesis*, **8**, 591–597.
22. Sumpter,W.C. and Miller,F.M. (1954) *The Chemistry of Heterocyclic Systems: Heterocyclic Compounds with Indole and Carbazole Systems*. Interscience Publishers, New York.
23. Buu-Hoi,N.P., Hoan,N. and Khoi,N.H. (1949) Carcinogenic derivatives of carbazole. I. The synthesis of 1,2,7,8-, 1,2,5,6- and 3,4,5,6-dibenzocarbazole and some of their derivatives. *J. Org. Chem.*, **14**, 492–497.
24. Fieser,L.F. and Fieser,M. (ed.) (1967) *Reagents for Organic Synthesis*, Wiley Interscience, New York, Vol. 1, pp. 66–67.
25. Fieser,M. and Fieser,L.F. (ed.) (1969) *Reagents for Organic Synthesis*, Wiley Interscience, New York, Vol. 2, pp. 33–34.
26. Stevens,T.S. and Tucker,S.H. (1923) The preparation of *N*-derivatives in the carbazole series. *J. Chem. Soc.*, **123**, 2140–2147.
27. Seglen,P.O. (1976) Preparation of isolated rat liver cell. *Methods Cell Biol.*, **13**, 29–83.
28. Holm-Hansen,O. and Karl,D.M. (1978) Biomass and adenylate energy charge determination in microbial cell extracts and environmental samples. *Methods Enzymol.*, **57**, 73–85.
29. Burton,K. (1968) Determination of DNA concentration with diphenylamine. *Methods Cell Biol.*, **12(B)**, 163–166.
30. DePierre,J.W., Moron,M.S., Johannesen,K.A.M. and Ernster,L. (1975) A reliable, sensitive, and convenient radioactive assay for benzpyrene monooxygenase. *Anal. Biochem.*, **63**, 470–484.
31. VanCantfort,J., DeGraeve,J. and Gielen,J.E. (1977) Radioactive assay for aryl hydrocarbon hydroxylase. *Biochem. Biophys. Res. Commun.*, **79**, 505–512.
32. Yerganian,G., Nell,M.A., Cho,S.S., Hayford,A.H. and Ho,T. (1968) Virus-associated gain and loss of proliferative and neoplastic properties of normal and virus-transformed diploid cell lines. *Natl. Cancer Inst. Monogr.*, **29**,

241–268.
33. Dooley,J. (1984) Mutagenesis of polycyclic aromatic hydrocarbons and *N*-heterocyclic aromatics in the Chinese hamster DPI-3 epithelial cell line. Ph.D. Thesis, University of Cincinnati, Kettering Laboratory.
34. Snee,R.D. and Irr,J.D. (1981) Design of a statistical method for the analysis of mutagenesis at the hypoxanthine-guanine phosphoribosyl transferase locus of cultured Chinese hamster ovary cells, *Mutat. Res.*, **85**, 77–93.
35. Su,H. (1981) Statistical evaluation of mutagenicity in the DPI-3/HGPRT marker mammalian cell system. M.S. Thesis, University of Cincinnati, Kettering Laboratory.
36. Gill,J.H., Duke,C.C. Rosario,C.A., Ryan,A.J. and Holder,G.M. (1986) Dibenz[*a,j*]acridine metabolism: identification of *in vitro* products formed by liver microsomes from 3-methylcholanthrene-pretreated rats. *Carcinogenesis*, **7**, 1371–1378.
37. Warshawsky,D., Hollingsworth,L., Reilman,R. and Stong,D. (1985) The metabolism of dibenz[*a,j*]acridine in the isolated perfused lung. *Cancer Lett.*, **28**, 317–326.
38. Gelboin,H.V. (1980) Benzo[*a*]pyrene metabolism, activation, and carcinogenesis: role and regulation of mixed-function oxidases and related enzymes. *Physiological Rev.*, **60**, 1107–1166.
39. Tomaszewski,J.E., Jerina,D.M. and Daly,J.W. (1975) Deuterium isotope effects during formation of phenols by hepatic monooxygenases. Evidence for an alternative to the arene oxide pathway. *Biochemistry*, **14**, 2024–2031.
40. Perin,F., Valero,D., Thybaud-Lambay,V., Plessis,M.J. and Zajdela,F. (1988) Organ-specific, carcinogenic dibenzo[*c,g*]carbazole derivatives: discriminative response in *S.typhimurium* TA100 mutagenesis modulated by subcellular fractions of mouse liver. *Mutat. Res.*, **198**, 15–26.
41. Perin,F., Valero,D., Mispelter,J. and Zajdela,F. (1984) *In vitro* metabolism of *N*-methyl-benzo[*c,g*]carbazole, a potent sarcomatogen devoid of hepatotoxic and hepatocarcinogenic properties. *Chem.-Biol. Interact.*, **48**, 281–295.

Received on August 12, 1986; revised on April 14, 1987; accepted on December 8, 1988